16. Stanton, M. R., Wanty, R. B., Lawrence, E. P. and Briggs, P. H., Dissolved radon and uranium, and ground-water geochemistry in an area near Hylas, Virginia. US Geological Survey Bulletin, 2070, 1996.
17. Krishnaswami, S., Graustein, W. C., Turekian, K. K. and Dowd, J. F., Radium, thorium, and radioactive lead isotopes in groundwaters: application to the *in situ* determination of adsorption–desorption rate constants and retardation factors. *Water Resour. Res.*, 1982, **18**, 1663–1675.
18. Kozowska, B., Walencik, A., Dorda, J. and Zipper, W., Radon in groundwater and dose estimation for inhabitants in spas of the Sudety Mountain area, Poland. *Appl. Radiat. Isot.*, 2010, **68**, 854–857.
19. Zouridakis, N., Ochsenkühn, K. M. and Savidou, A., Determination of uranium and radon in potable water samples. *J. Environ. Radioact.*, 2002, **61**(2), 225–232.
20. Horvath, A, Bohus, L. O., Urbani, F., Marx, G., Piroth, A. and Greaves, E. D., Radon concentrations in hot spring waters in northern Venezuela. *J. Environ. Radioact.*, 2000, **47**, 127–133.
21. Skeppstrom, S. and Olofsson, B., Uranium and radon in groundwater, an overview of the problem, *Eur. Water*, 2007, **17/18**, 51–62.
22. Abdallaha Samer, M., Habibb Rima, R., Nuwayhida Rida, Y., Malek, C. and Gabriel, K., Radon measurements in well and spring water in Lebanon. *Radiat. Meas.*, 2007, **42**, 298–303.
23. Leo, M., Savio, S., Tom, R. and Tony, C., Radon in drinking water in country Wicklow – a pilot study. In Diffuse Pollution Conference Dublin, 2003, 8B, Ecology.
24. Han, Y. L., Tom Kuo, M. C., Fan, K. C., Chiang, C. J. and Lee, Y. P., Radon distribution in groundwater of Taiwan. *Hydrogeol. J.*, 2006, **14**, 173–179.
25. Choubey, V. M., Batarya, S. K. and Romola, R. C., Radon in groundwater of eastern Doon valley, Outer Himalaya. *Radiat. Meas*., 2003, **36**, 401–405.
26. King, P. T., Discussion of Radon distribution in domestic water of Texas by Irina Cech, Charles Kreitler, Howard Prichard, Alfonso Holguin and Mengistu Lemma. *Ground Water*, 1989, **26**, 561–569.
27. Rama, Moore, W. S., Mechanism of transport of U–Th series radioisotopes from solids into groundwater. *Geochim. Cosmochim. Acta*, 1984, **48**, 395–399.
28. Davidson, M. R. and Dickson, B. L., A porous flow model for steady state transport of radium in groundwater. *Water Resour. Res*., 1986, **22**, 34–44.
29. Andrews, J. N., Ford, D. J., Hussain, N., Trivedi, D. and Youngman, M. J., Natural radioelement solution by circulating groundwaters in the Stripa granite. *Geochim. Cosmochim. Acta*, 1989, **53**, 1791–1802.
30. Loomis, D. P., Radon-222 concentration and aquifer lithology in North Carolina. *Ground Water Monit. Rev*., 1987, **7**(2), 33–39.
31. King, P. T., Michel, J. and Moore, W. S., Ground water geochemistry of ^{228}Ra, ^{226}Ra and ^{222}Rn. *Geochem. Cosmochim. Acta*, 1982, **46**, 1173–1182.
32. UNSCEAR, Report to the General Assembly, 2000.
33. WHO, *Guidelines for Drinking Water*, 2004, vol. 1, 3rd edn.
34. Nazaroff, W. W., Doyle, S. M., Nero, A. V. and Sextro, R. G., Notable water as a source of airborne ^{222}Rn in US dwellings: review and assessment. *Health Phys*., 1987, **52**(3), 281–295.
35. Kendall, G. M. and Smith, T. J., Doses to organs and tissues from radon and its decay products. *J. Radiol. Prot.*, 2002, **22**, 389–406.
36. Shiva Prasad, N. G., Nagaiah, N., Ashok, G. V. and Mahesh, H. M., Radiation dose from dissolved radon in potable waters of the Bangalore environment, South India. *Int. J. Environ. Stud.*, 2007, **64**, 83–92.

ACKNOWLEDGEMENT. We thank Dr K. S. Pradeep Kumar (BARC, Mumbai), for guidance and support during this study.

Received 7 April 2015; revised accepted 15 July 2015

doi: 10.18520/v109/i10/1855-1860

Development of hydrophobic platinum-doped carbon aerogel catalyst for hydrogen–deuterium exchange process at high pressure

Rashmi Singh[1], M. K. Singh[1,*], D. K. Kohli[1], Ashish Singh[1], Sushmita Bhartiya[1], A. K. Agarwal[2] and P. K. Gupta[1]

[1]Nano Functional Materials Laboratory,
Laser Materials Development and Devices Division,
Raja Ramanna Centre for Advanced Technology, Indore 452 013, India
[2]Heavy Water Board, Vikram Bhawan, Anushakti Nagar,
Mumbai 400 094, India

The use of catalysed exchange of deuterium (D) between hydrogen (H) gas and liquid water using the bithermal hydrogen water (BHW) process is a promising and environment-friendly approach for the production of heavy water. However, the use of this approach is limited by the lack of a suitable catalyst that has good activity at high operating pressures required for practical applications. We report the development of hydrophobic platinum-doped carbon aerogel (PtCA) catalyst which shows good catalytic activity for H/D isotope exchange reactions at operating pressures up to 20 bar.

Keywords: Carbon dioxide activation, hydrogen isotope separation, hydrophobic catalyst, platinum-doped carbon aerogel.

CATALYSED exchange of deuterium (D) between hydrogen (H) gas and liquid water (liquid phase catalytic exchange (LPCE) reaction) using bi-thermal hydrogen water (BHW) process is receiving considerable attention for heavy water production[1]. This is because it is more energy-efficient and environment-friendly compared to the existing 'girder sulphide' and 'ammonia–hydrogen' processes. The catalysed exchange involves two steps – first, deuterium exchange between hydrogen gas and water vapour at the catalytic site and subsequently equilibration of deuterated water vapour with liquid water at gas–liquid interface, which results in the transfer of deuterium from gas to liquid phase. Success of the process requires simultaneous presence of H_2 gas and water vapour at the catalytic site and easy accessibility of liquid water to water vapour involved in isotopic exchange reaction. However, because the solubility of H_2 gas in water is poor, if the catalytic site is covered with liquid water, the exchange of deuterium between hydrogen gas and water vapour is highly impeded[2]. Therefore, a primary requirement for the LPCE process is that the catalyst should allow access of gaseous reactants to the catalytic

*For correspondence. (e-mail: singhmk@rrcat.gov.in)

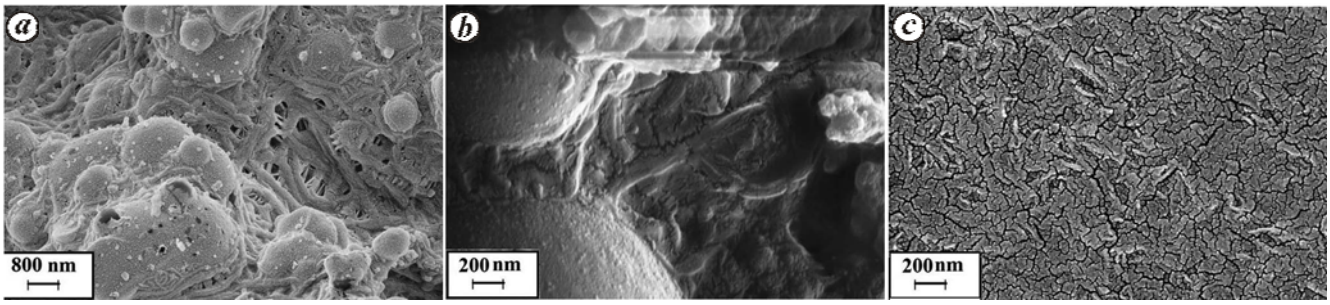

Figure 1. SEM image of catalyst with PTFE film at (***a***) M : 25,000; (***b***) M : 100,000 and (***c***) SEM image of perfluoroalkoxyalkanes coating at M : 100,000.

Table 1. Textural properties of carbon aerogels

Material	Total surface area (m^2/g)	Mesopore surface area (m^2/g)	Maxima of pare size distribution (nm)
Carbon aerogel	698	289	8.6
CO_2-activated carbon aerogel	1647	547	7

site, and should have a hydrophobic surface so that water does not cover the catalytic sites[3]. Further, for a high throughput for the LPCE process, it is desirable that the catalyst should remain active at high pressure so that water remains in the liquid phase at high temperature (130°C) of operation[4].

Since the first patent published by Stevens for hydrophobic catalyst in 1972, several efforts have been made for the development of wet-proof catalyst using different support materials (activated carbon, silica, nickel foam, etc.)[5,6], active metals (Pt, Ru, Rh, Ti, Cr, etc.)[7,8] and binders (polytetraflouroethylene (PTFE), emulsion coating, PTFE extrudes/thin films, styrenedivinylbenzene copolymer (SDBC) granules/coatings and silicone resins)[9]. However, these show good activity only up to atmospheric pressure and rapidly lose activity as the pressure is increased above atmospheric pressure. This has limited the use of the LPCE process for relatively low-throughput applications like removal of tritium from heavy water of the moderator used in pressurized heavy water reactor operation[10].

The reduction in catalyst activity at higher pressure is believed to arise due to ingression of water at such pressure through pores in the fibrous network or mesh structure of the commonly used hydrophobic binders like PTFE and SDBC. Indeed, the studies carried out by Malhotra *et al.*[11] showed how the size and distribution of pore in binder contribute to the loss of activity at higher pressure. To address this issue, we have explored different approaches like high-pressure melting of PTFE film, PTFE overcoat, coating of other binders like polyvinylidenedifluoride (PVDF), perfluoroalkoxyalkanes (PFA), etc. to control the porosity of the film. These studies have led us to the successful development of hydrophobic platinum-doped carbon aerogel (PtCA) catalyst that shows good catalytic activity even up to 20 bar.

In our earlier studies we had mixed PtCA powder synthesized by *in situ* sol–gel polymerization method with colloidal PTFE solution and coated on Dixon rings to obtain the hydrophobic catalyst[12]. This catalyst showed good catalytic activity for hydrogen isotope exchange in atmospheric pressure conditions. However, the catalytic activity was observed to decrease rapidly as the operating pressure was increased above atmospheric pressure. Although attempts to control the porosity of the film by use of high-pressure melting of PTFE film did not succeed, coating of another hydrophobic binder PFA on PtCA/PTFE catalyst led to retention of activity at higher pressure. Figure 1 shows the SEM images (Carl Zeiss Sigma FESEM) of PTFE and PFA hydrophobic films coated on Dixon rings. Figure 1 *a* shows fibrous/mesh structure with small opening of the order of 400–500 nm in PTFE film. Further magnified image of these films (Figure 1 *b*) shows cracks in them, which may be due to the low viscosity of PTFE in molten state. In contrast, the catalyst having a coating of PFA on PTFE film (Figure 1 *c*) shows a continuous void-free surface morphology and the average pore diameter is of the order of 10–12 nm. This may be because of the lower viscosity and melt flowable property of PFA.

However, with additional coating of PFA over PTFE film, the catalytic activity measured in terms of column efficiency of the isotopic exchange at 35°C and atmospheric pressure reduced from ~ 30% to ~10%.

An improvement in the activity of the catalyst can be achieved by improving the surface area of the catalyst and dispersion of Pt in it. With this objective we carried out CO_2 activation at high temperature (~900°C) of carbon aerogel (CA) prepared using the method described in our earlier work[13]. Table 1 summarizes the textural properties of carbon aerogel and CO_2-activated carbon aerogel (ACA) determined using surface area analyser (Micromeritics, ASAP2020). CO_2 activation increases total surface area and mesopore surface area.

For loading Pt in CA, hexachloroplatinic acid was dissolved in ethylene glycol and then impregnated on carbon aerogel by microwave-assisted polyol process, which is known to be an efficient method for dispersion of Pt nanoparticles in carbon support[14]. Figure 2 shows TEM images (Philips, CM200) of the Pt-impregnated CA and ACA powder. On CO_2-activated carbon aerogel (Figure 2 *a*), well-dispersed platinum with average cluster size 2.4 nm can be seen. In contrast, a very broad particle size distribution with average platinum cluster size of 5.2 nm is obtained for carbon aerogel without activation (Figure 2 *b*).

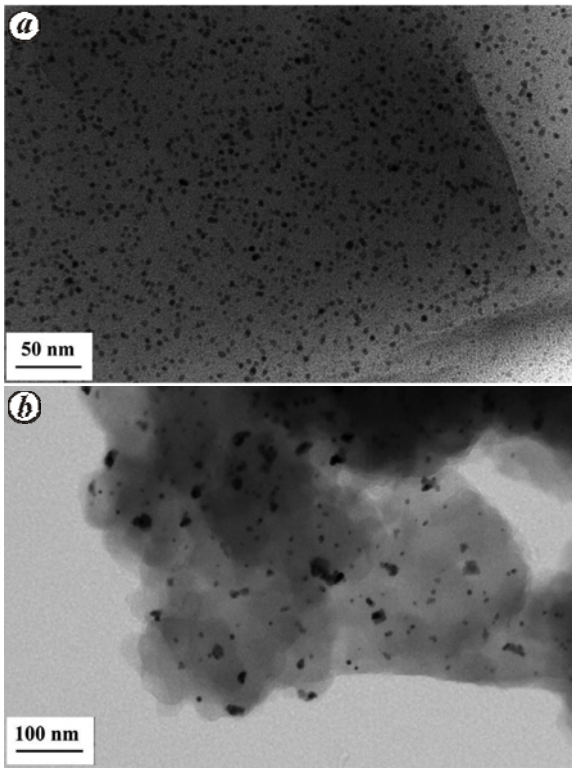

Figure 2. (***a***) TEM image of Pt on (***a***) CO_2-activated carbon aerogel (ACA) and (***b***) carbon aerogel.

CO_2 activation of carbon aerogel not only leads to an increase in the surface area, but also to an increase in defects sites. Evidence for the latter was provided by the observed increase in the intensity of the 1348 cm^{-1} D band of the Raman spectra of ACA (Figure 3). These factors may contribute to the observation of better Pt dispersion in ACA[15].

Figure 4 shows the XRD powder diffraction (Rigaku) spectra of both the samples. The very broad peak for Pt ACA is indicative of smaller Pt particle size. The average size of the Pt particles determined by Scherer formula based on Pt(111) peak was 1.8 nm for Pt ACA as against 4.2 nm for CA without activation.

Chemisorption of hydrogen on Pt surfaces was also carried out as it provides the most reliable data concerning true concentrations of active Pt surface sites on supported catalyst compared to those estimated from particle size measured by TEM and XRD. The chemisorption results using hydrogen gas show Pt dispersion of 17.6% for CA and 36% for ACA; the estimates for Pt particle size using dispersion values were 6.3 and 3.1 nm respectively. All these measurements confirm that better dispersion of platinum is achieved in CO_2-activated carbon aerogel.

Performance of the catalyst prepared using PFA binder on PTFE/PtACA was tested for H/D exchange reactions in a high-pressure–high-temperature testing column. Deuterated water (~700 ppm HDO) was fed at the top of the column and natural hydrogen gas (~50 ppm HD) was fed from the bottom. Isotope exchange takes place between water and gas which are flowing in counter current manner in the reaction column. The catalytic performance was

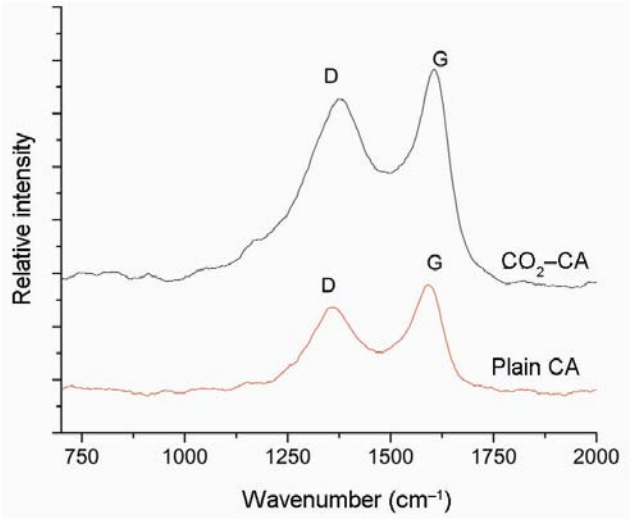

Figure 3. Raman spectra of CA and ACA.

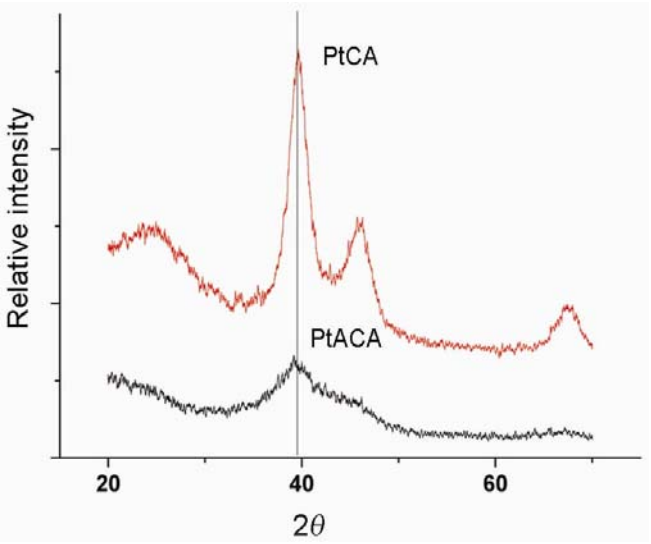

Figure 4. XRD spectra of Pt on CO_2-activated CA and Pt on CA.

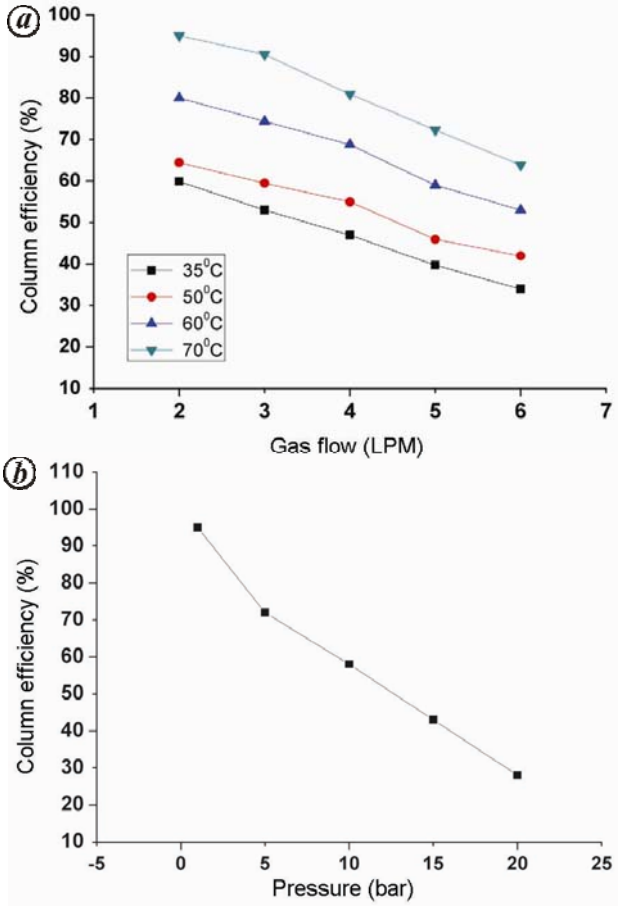

Figure 5. ***a***, Column efficiency at different values of temperature and H_2 gas flow. ***b***, Column efficiency at different values of pressure.

evaluated using the column efficiency of the isotopic exchange column (η) expressed as

$$\eta = (y_t - y_b)/(y_e - y_b),$$

where y_b is the HD concentration in the hydrogen gas at the bottom, y_t the HD concentration in the hydrogen gas on the top of the column and y_e is the HD equilibrium concentration in the hydrogen gas at the outlet[16]. The column efficiencies were measured at temperatures varying from 35°C to 70°C and for varying gas flows and pressures. The results are shown in Figure 5 *a*. At atmospheric pressure and H_2 flow rate of 2 lpm, efficiencies of 60% at 35°C and 95% at 70°C were obtained. These values compare favourably with previous reports where at 70°C under similar gas flow conditions, efficiencies varying from 75% to 85% have been reported[8,17]. The increase in exchange efficiency with increase in temperature is expected because the increase in water vapour pressure at higher temperature helps H/D catalytic reaction between water vapour and H_2 gas. The catalyst was tested for values above the atmospheric pressure up to 20 bar at 70°C. Figure 5 *b* shows the measured catalytic activity as a function of pressure. Efficiency can be seen to reduce from 95% at atmospheric pressure to 21% at 20 bar. After operation at pressure of 20 bar, when the same catalyst was again tested at atmospheric pressure, no degradation in the activity was observed. These results suggest that high pressure operation does not lead to loss of hydrophobicity and that the observed decrease in efficiency on increasing the pressure is due to decrease in wt.% water vapour content with increase in pressure.

To conclude, we have demonstrated that an appropriate coating of PFA on PTFE /PtCA-coated catalyst leads to a continuous void-free structure, which helps achieve good catalytic activity for the LPCE process even up to 20 bar.

1. Dave, S. M., Sadhukhan, H. K. and Novaro, O. A., *Heavy Water Properties, Production and Analysis*, Quest Publication, Mumbai, India, 1st edn, 1997.
2. Butler, J. P. and Hartog, J. D., Process for the exchange of hydrogen isotopes using a catalyst packed bed assembly, US Patent No. 4126667, 1978.
3. Stevens, W. H., Process for hydrogen isotope exchange and concentration between liquid water and hydrogen gas and catalyst assembly therefor. US Patent No. 3888974, 1975.
4. Masami, S., Ryohei, N. and Asashi, K., Dual temperature dual pressure isotopic exchange reaction method. Canadian Patent No. 1170818, 1981.
5. Butler, J. P., Rolston, J. H. and Hartog, J. D., Catalytically active mass for the exchange of hydrogen isotopes between streams of gaseous hydrogen and liquid water. US Patent No. 4228034, 1980.
6. Hu, S., Hou, J., Xiong, L., Weng, K., Ren, X. and Luo, Y., Preparation and characterization of hydrophobic Pt–Fe catalysts with enhanced catalytic activities for interface hydrogen isotope separation. *J. Hazard. Mater.*, 2012, **209–210**, 478–483.
7. Ye, L., Luo, D., Yang, W., Guo, W., Xu, Q. and Luo, L., Preparation and characterization of hydrophobic carbon-supported Pt 3*M* (*M* = Fe, Co, Ni and Cr) bimetals for H/D isotope separation between hydrogen and water. *Int. J. Hydrogen Energy*, 2014, **39**(25), 13793–13799.
8. Hu, S., Xiong, L., Hou, J., Weng, K., Luo, Y. and Yang, T., The roles of metals and their oxide species in hydrophobic Pt–Ru catalyst for the interphase H/D isotope separation. *Int. J. Hydrogen Energy*, 2010, **35**, 10118–10126.
9. Huang, F. and Meng, C., Hydrophobic platinum–polytetrafluroethylene catalyst for hydrogen isotope separation. *Int. J. Hydrogen Energy*, 2010, **35**, 6108–6112.
10. Popescu, I., Ionita, Gh., Stefanescu, I., Varlam, C., Dobrinescu, D. and Faurescu, I., Improved characteristics of hydrophobic polytetrafluroethylene–platinum catalyst for tritium recovery from tritiated water. *Fusion Eng. Des.*, 2008, **83**, 1392–1394.
11. Malhotra, S. K., Krishnan, M. S. and Sadhukhan, H. K., Development of hydrophobic catalyst for hydrogen isotope exchange between hydrogen gas and liquid water, In Proceedings of the National Symposium on Heavy Water Technology, Mumbai, 1989.
12. Singh, M. K., Singh, R., Singh, A., Kohli, D. K., Deshpande, U. and Gupta, P. K., Preparation and characterization of hydrophobic platinum-doped carbon aerogel catalyst for hydrogen isotope separation. *Bull. Mater. Sci.*, 2014, **37**, 1–4.
13. Kohli, D. K., Singh, R., Singh, A., Bhartiya, S., Singh, M. K. and Gupta, P. K., Enhanced salt-adsorption capacity of ambient pressure-dried carbon aerogel activated by CO_2 for capacitive deionization application. *Desalination Water Treatment*, 2015, **54**, 2725–2731.

14. Chu, Y., Wang, Z., Gu, D. and Yin, G., Performance of Pt/C catalysts prepared by microwave-assisted polyol process form ethanol electrooxidation. *J. Power Sources*, 2010, **195**, 1799–1804.
15. Vinayan, B. P., Nagar, R., Rajalakshmi, N. and Ramaprabhu, S., Novel platinum–cobalt alloy nanoparticles dispersed on nitrogen-doped grapheme as a cathode electrocatalyst for PEFMC applications. *Adv. Funct. Mater*., 2012, **22**, 3519–3526.
16. Hu, S., Xiong L., Ren, X., Wang, C. and Luo, Y., Pt–Ir binary hydrophobic catalyst: effects of Ir content and particle size on catalytic performance for liquid phase catalytic exchange. *Int. J. Hydrogen Energy*, 2009, **34**, 8723–8732.
17. Ye, L., Luo, D., Yang, W., Guo, W., Xu, Q. and Jiang, C., Improved catalysts for hydrogen/deuterium exchange reactions. *Int. J. Hydrogen Energy*, 2013, **38**, 13596–13603.

ACKNOWLEDGEMENTS. We thank Shri Tulsiram, Shri B. P. Dubey, P Kumawat (Heavy Water Plant, Baroda) for carrying out the catalytic activity measurements and Shri Rajnish Prakash (Heavy Water Board) for encouragement and support. We also thank Shri Gopal Mohod (RRCAT, Indore) for assistance.

Received 1 May 2015; revised accepted 30 July 2015

doi: 10.18520/v109/i10/1860-1864

Gravitational attraction of a vertical pyramid model of flat top and bottom with depth-wise linear density variation

Anand P. Gokula and Rambhatla G. Sastry*

Department of Earth Sciences, Indian Institute of Technology, Roorkee 247 667, India

In 3D gravity modelling, a right rectangular parallelepiped with either constant density or variable density functions in spatial and spectral domains enjoys wide popularity. However, better unit models are needed to meet the large variety of geological scenarios. Here, we present an analytical expression for the gravity effect of a vertical pyramid model with depth-wise linear density variation. Initially, we validate our analytic expression against the gravity effect of a right rectangular parallelepiped and provide two synthetic examples and a case study for illustrating the effectiveness of our pyramid model in gravity modelling. The included case study of Los Angeles basin, California, USA, demonstrates the comparative advantages of our pyramid model over the conventional right rectangular vertical prism model. Thus, our pyramid model could be quiet effective as a building block for evaluating the gravity effect of an arbitrarily-shaped 3D or 2.5D source(s).

Keywords: Gravitational attraction, linear density variation, right rectangular, parallelepiped model, vertical pyramid model.

THE evaluation of theoretical gravity response of 3D targets is an involved process requiring considerable theoretical and computational efforts. Several authors have addressed this problem in both spatial[1–4] and spectral domains[5,6]. The polygonal lamina model[4], the right rectangular prism model with constant density contrast[1,3], and the right rectangular prism model with parabolic density variation depth-wise[2] have enjoyed wide popularity. However, for real geological applications, one needs better 3D unit models.

Starostenko[7] has proposed an inhomogeneous vertical pyramid model with flat top and bottom and sloping sides possessing a linear density variation depth-wise. However, he was unable to derive a complete analytical expression for its gravity effect.

Here, we derive the complete gravity expression for the same pyramid model and illustrate its effectiveness through two synthetic examples after customary validation check of our forward problem solution.

Consider an isolated regular pyramid model *ABCDEFGH* with flat top *ABCD* and bottom surface, EFGH (Figure 1 *a*). The gravity effect of such a model at any arbitrary point (x, y, z) in free space[7] is given by

$$g_{\text{pyramid}}(x, y, z) = \gamma \int_{\zeta=h_1}^{h_2} \int_{\eta=\eta_l}^{\eta_u} \int_{\xi=\xi_l}^{\xi_u} \frac{\sigma(\zeta)(\zeta - z)\mathrm{d}\xi\mathrm{d}\eta\mathrm{d}\zeta}{((\xi - x)^2 + (\eta - y)^2 + (\zeta - z)^2)^{3/2}}, \quad (1)$$

where

$$\left.\begin{aligned} \sigma(\zeta) &= \sigma + k(\zeta - h_1), \\ \xi_l &= (h_1 - \zeta)(\xi_1 - \xi_3)/(h_2 - h_1) + \xi_1, \\ \xi_u &= (h_1 - \zeta)(\xi_2 - \xi_4)/(h_2 - h_1) + \xi_2, \\ \eta_l &= (h_1 - \zeta)(\eta_1 - \eta_3)/(h_2 - h_1) + \eta_1, \\ \eta_u &= (h_1 - \zeta)(\eta_2 - \eta_4)/(h_2 - h_1) + \eta_2. \end{aligned}\right\}, \quad (2)$$

where σ is constant density (g/cm^3), k the linear coefficient (g/cm^3/km), γ the universal gravitational constant, h_1 and h_2 are the depth of the top and bottom surfaces of pyramid respectively, and ζ refers to depth below h_1. $A(\xi_1, \eta_1, h_1)$, $B(\xi_1, \eta_2, h_1)$, $C(\xi_2, \eta_2, h_1)$, $D(\xi_2, \eta_1, h_1)$, $E(\xi_3, \eta_3, h_2)$, $F(\xi_3, \eta_4, h_2)$, $G(\xi_4, \eta_4, h_2)$ and $H(\xi_3, \eta_3, h_2)$ are the corners of the pyramid (Figure 1 *a*). By changing

*For correspondence. (e-mail: rgss1fes@iitr.ac.in)